Fermilab FERMILAB-Pub-00/024-E E791 September 2000

Asymmetries in the production of Λ^0, Ξ^-, and Ω^- hyperons in 500 GeV/c π^- – Nucleon Interactions

Fermilab E791 Collaboration

E. M. Aitala,[i] S. Amato,[a] J. C. Anjos,[a] J. A. Appel,[e]
D. Ashery,[n] S. Banerjee,[e] I. Bediaga,[a] G. Blaylock,[h]
S. B. Bracker,[o] P. R. Burchat,[m] R. A. Burnstein,[f] T. Carter,[e]
H. S. Carvalho,[a] N. K. Copty,[l] L. M. Cremaldi,[i] C. Darling,[r]
K. Denisenko,[e] S. Devmal,[c] A. Fernandez,[k] G. F. Fox,[l]
P. Gagnon,[b] C. Gobel,[a] K. Gounder,[i] A. M. Halling,[e]
G. Herrera,[d] G. Hurvits,[n] C. James,[e] P. A. Kasper,[f]
S. Kwan,[e] D. C. Langs,[l] J. Leslie,[b] B. Lundberg,[e] J. Magnin,[a]
S. MayTal-Beck,[n] B. Meadows,[c] J. R. T. de Mello Neto,[a]
R. H. Milburn,[p] J. M. de Miranda,[a] A. Napier,[p] A. Nguyen,[g]
A. B. d'Oliveira,[c,k] K. O'Shaughnessy,[b] K. C. Peng,[f]
L. P. Perera,[c] M. V. Purohit,[l] B. Quinn,[i] S. Radeztsky,[q]
A. Rafatian,[i] N. W. Reay,[g] J. J. Reidy,[i] A. C. dos Reis,[a]
H. A. Rubin,[f] D. A. Sanders,[i] A. K. S. Santha,[c]
A. F. S. Santoro,[a] A. J. Schwartz,[c] M. Sheaff,[d,q]
R. A. Sidwell,[g] F. R. A. Simão,[a] A. J. Slaughter,[r]
M. D. Sokoloff,[c] J. Solano,[a] N. R. Stanton,[g] K. Stenson,[q]
D. J. Summers,[i] S. Takach,[r] K. Thorne,[e] A. K. Tripathi,[g]
S. Watanabe,[q] R. Weiss-Babai,[n] J. Wiener,[j] N. Witchey,[g]
E. Wolin,[r] D. Yi,[i] S. Yoshida,[g] R. Zaliznyak,[m] C. Zhang[g]

[a] *Centro Brasileiro de Pesquisas Físicas, Rio de Janeiro, Brazil*

[b] *University of California, Santa Cruz, California 95064, USA*

[c] *University of Cincinnati, Cincinnati, Ohio 45221, USA*

[d] *CINVESTAV, Mexico*

[e] *Fermilab, Batavia, Illinois 60510, USA*

[f] *Illinois Institute of Technology, Chicago, Illinois 60616, USA*

[g] *Kansas State University, Manhattan, Kansas 66506, USA*

[h] *University of Massachusetts, Amherst, Massachusetts 01003, USA*

[i] *University of Mississippi–Oxford, University, MS 38677, USA*
[j] *Princeton University, Princeton, New Jersey 08544, USA*
[k] *Universidad Autonoma de Puebla, Mexico*
[l] *University of South Carolina, Columbia, South Carolina 29208, USA*
[m] *Stanford University, Stanford, California 94305, USA*
[n] *Tel Aviv University, Tel Aviv 69978, Israel*
[o] *Box 1290, Enderby, British Columbia V0E 1VO, Canada*
[p] *Tufts University, Medford, Massachusetts 02155, USA*
[q] *University of Wisconsin, Madison, Wisconsin 53706, USA*
[r] *Yale University, New Haven, Connecticut 06511, USA*

Abstract

Using data from Fermilab fixed-target experiment E791, we have measured particle-antiparticle production asymmetries for Λ^0, Ξ^-, and Ω^- hyperons in π^- – nucleon interactions at 500 GeV/c. The asymmetries are measured as functions of Feynman-x (x_F) and p_T^2 over the ranges $-0.12 \leq x_F \leq 0.12$ and $0 \leq p_T^2 \leq 4(GeV/c)^2$. We find substantial asymmetries, even at $x_F = 0$. We also observe leading-particle-type asymmetries which qualitatively agree with theoretical predictions.

Strange particle production is an important tool for studying how non-perturbative QCD affects light quark production and hadronization. One process that involves both production and hadronization is the leading particle effect. This effect is manifest as an enhancement in the production rate of particles which have one or more valence quarks in common with an initial state hadron compared to that of their antiparticles which have fewer valence quarks in common. This enhancement increases as the momentum of the produced particle increases, in the direction of the initial hadron with which the produced particle shares valence quarks. This process has been extensively studied in charm production in recent years from both experimental [1,2] and theoretical [3] points of view. The same type of leading particle effects have been seen in light hadron production [4] and are expected [5]. Other effects, like the associated production of a kaon and a hyperon, can also contribute to an asymmetry in hyperon-antihyperon production [6].

As a byproduct of our charm program in Fermilab experiment E791, we collected a large sample of $\Lambda^0 - \overline{\Lambda}^0$, $\Xi^- - \Xi^+$, and $\Omega^- - \Omega^+$ hyperons which we have used to measure the particle-antiparticle production asymmetries reported here. For hyperons, the range of scaled longitudinal momentum x_F ($2p_L/\sqrt{s}$) covered by our experiment was $-0.12 \leq x_F \leq 0.12$. Given E791's negative pion beam and nucleon target, we expect recombination effects [5]

to produce different asymmetries in the beam and target fragmentation regions as the content of valence quarks in the beam and target hadrons differ. A growing asymmetry is expected in $\Lambda^0 - \overline{\Lambda}^0$ production as $|x_F|$ increases in the negative direction towards the target fragmentation region. A smaller asymmetry (or none at all) is expected for $x_F > 0$, towards the beam fragmentation region, because Λ^0 and $\overline{\Lambda}^0$ each share one valence quark with the incident pion. For $\Xi^- - \Xi^+$ production, a growing asymmetry with $|x_F|$ is expected in both regions since the Ξ^- shares one valence quark with the π^- as well as with the target particles (p and n) whereas the Ξ^+ shares none. No leading particle effects are expected for Ω^- or Ω^+ as they have no valence quarks in common with either the target or the beam.

Measurements of $\Lambda^0 - \overline{\Lambda}^0$ [7], $\Xi^- - \Xi^+$, and $\Omega^- - \Omega^+$ [8] production asymmetries in π^-Cu interactions at 230 GeV/c have been reported in the literature. Additional measurements of the $\Lambda^0 - \overline{\Lambda}^0$ asymmetry can be found in the experiments listed in [9], but in general light hadron production asymmetries in $\pi^- N$ interactions have not been studied extensively.

Experiment E791 recorded data from 500 GeV/c π^- interactions in five thin foils (one platinum and four diamond) separated by gaps of 1.38 to 1.39 cm. Each foil had a thickness of approximately 0.4% of a pion interaction length (0.5 mm for the upstream platinum target, and 1.6 mm for each of the carbon targets). The E791 spectrometer [10] in the Fermilab Tagged Photon Laboratory was a large-acceptance, two-magnet spectrometer augmented by eight planes of multiwire proportional chambers (MWPC) and six planes of silicon microstrip detectors (SMD) for beam tracking. The magnets provided a total transverse momentum kick of 512 MeV/c. Downstream of the target there were 17 planes of SMD's for track and vertex reconstruction, 35 drift chamber planes, two MWPC's, two multicell threshold Čerenkov counters, electromagnetic and hadronic calorimeters (with apertures about 70 by 140 mr), and a muon detector. An important element of the experiment was its extremely fast data acquisition system [11] which was combined with a very open transverse-energy trigger to record a data sample of 2×10^{10} events. The trigger required that the total "transverse energy" (i.e., sum of the products of energy observed times the tangent of the angle from the target to each calorimeter segment) be at least 3 GeV.

For this analysis we use only interactions in the isoscalar carbon targets so that our results truly represent a "nucleon", that is, the average of neutrons and protons. Most Λ^0's decay before entering the drift chamber region (150 cm downstream of the targets) but downstream of the end of the silicon vertex detectors (50 cm from the targets), while some Ξ^-'s and Ω^-'s decay in the silicon region.

Throughout this paper, references to a particle should be taken to include its

antiparticle unless explicitly stated otherwise. Λ^0's were reconstructed using the $p\pi^-$ decay mode. Proton and π^- tracks were required to have a distance of closest approach less than 0.7 cm at the decay vertex and to have an invariant mass between 1.101 and 1.127 GeV/c^2. In addition, the ratio of the momentum of the proton to that of the pion was required to be larger than 2.5. The reconstructed Λ^0 decay vertex formed by the two tracks was required to be downstream of the last target but upstream of the first magnet. For the Λ^0 production study, we removed Λ^0's coming from Ξ^- decay by requiring that the Λ^0 candidates have an impact parameter with respect to the primary vertex of less than 0.3 cm if decaying within the first 20 cm downstream of the target, and less than 0.4 cm otherwise. After these cuts, the remaining Ξ^- contamination was $\approx 1.5\%$, having negligible effect on the $\Lambda^0 - \overline{\Lambda}^0$ asymmetry. The reconstructed mass distributions for this sample, for each interval of x_F and p_T^2, were fit using a binned maximum likelihood method with a Gaussian signal plus a linear background. All bin widths were much larger than the experimental resolution of the variable binned. In the fit, the central reconstructed mass values and mass resolutions were fixed to values obtained from Monte Carlo simulation. Contamination from misidentified $K_s^0 \to \pi^+\pi^-$ decays provided a flat background in these distributions in the range shown, and produced a negligible effect on the fit numbers of Λ^0's. The reconstructed mass distributions for the entire sample are shown in Figs. 1(a) and (b). For the $\Lambda^0 - \overline{\Lambda}^0$ analysis we use data from approximately 7% of the overall sample recorded for the experiment. The total signal, taken as the sum of background subtracted signal in each bin, was $2\,587\,870 \pm 1\,780$ Λ^0's and $1\,690\,030 \pm 1\,500$ $\overline{\Lambda}^0$'s.

Ξ^- were selected via the decay mode $\Xi^- \to \Lambda^0\pi^-$ and Ω^- via the decay mode $\Omega^- \to \Lambda^0 K^-$. Beginning with a Λ^0 candidate, we added a third, distinct track as a possible pion or kaon daughter. All three tracks were required to have hits in the drift chamber region only. For these samples, we removed the requirement on the Λ^0 impact parameter. The invariant mass of the candidate hyperon (calculated from the known mass and measured momentum of the Λ^0, as determined by its two decay tracks, together with the third track) was required to be between 1.290 and 1.350 GeV/c^2 for the Ξ^- and between 1.642 and 1.702 GeV/c^2 for the Ω^-. The charged hyperon track, entirely in the SMD region, was required to be reconstructed. Its direction had to match that determined by its daughter tracks in the drift chamber region to within 1 mrad and it was required to have a distance of closest approach to the primary vertex of less than 100 μm. The Ξ^- or Ω^- vertex (reconstructed from the Λ^0 and daughter π^- or K^-) was required to be downstream of the last SMD plane and upstream of the Λ^0 vertex. The former requirement allows us to track the hyperon in the silicon. For the Ω^- sample, the third track was required to have a kaon signature in the Čerenkov counters and momentum in the range 6-40 GeV/c. For this momentum range, the Čerenkov kaon identification efficiency

was about 85% and the pion misidentification rate was about 5%.

As with the Λ^0 sample, the $\Xi^- - \Xi^+$ and $\Omega^- - \Omega^+$ invariant mass plots were fit to a Gaussian signal plus linear background for each interval of x_F and p_T^2. The total reconstructed mass distributions are shown in Figs. 1(c) through (f). With the final selection criteria and the full E791 data set, we found $996\,180 \pm 1\,200$ Ξ^-, $706\,620 \pm 1\,020$ Ξ^+, $8\,750 \pm 110$ Ω^-, and $7\,460 \pm 100$ Ω^+ after background subtraction. Again, these numbers and their errors come from the sum of signals in all bins. We checked that the Ξ^- contamination for the Ω^-'s, after all cuts, was negligible.

For each x_F and p_T^2 bin and for each hyperon Y, we defined an asymmetry parameter A as

$$A_{Y-\overline{Y}} \equiv \frac{N_Y - N_{\overline{Y}}\, r_Y}{N_Y + N_{\overline{Y}}\, r_Y} \quad ; \quad r_Y = \frac{\epsilon_Y}{\epsilon_{\overline{Y}}}, \tag{1}$$

where N_Y ($N_{\overline{Y}}$) is the number of hyperons (antihyperons) produced in the bin, and ϵ_Y ($\epsilon_{\overline{Y}}$), the product of the geometrical acceptance and reconstruction efficiency for each hyperon (antihyperon). Values for the N's were obtained from the individual fits to the mass plots for events selected to lie within each x_F and p_T^2 range.

Selection criteria for the particle and antiparticle samples were identical. However, geometrical acceptances and reconstruction efficiencies were not necessarily the same, mostly due to an inefficient region in the drift chambers produced by the negative pion beam. To evaluate this effect, a large sample of Monte Carlo (MC) events was created using the PYTHIA/JETSET event generators [12]. These were projected through a detailed simulation of the E791 spectrometer to simulate "data" in digitized format which was then processed through the same computer reconstruction code as that used for data from the detector. Candidate events were then subjected to the same selection criteria as that used for data. To account for correlations between x_F and p_T^2, efficiencies were determined in bins of the two parameters. The ratios of efficiencies $\epsilon_Y/\epsilon_{\overline{Y}}\,(x_F, p_T^2)$ evaluated from the MC samples are shown for each hyperon in Figs. 2(a)–(c). For the x_F range of our data, there are only minor differences between particle and antiparticle efficiencies. This result was expected, as hyperon decays with tracks aimed at the inefficient part of the drift chambers were rare. As a further check, we verified that our results were not significantly affected by symmetrically eliminating these events.

The asymmetries obtained using Eq. 1 are shown in Figs. 3 and 4 for the hyperons Λ^0, Ξ^-, and Ω^-, as a function of x_F and p_T^2, respectively. For each hyperon the asymmetry is presented as functions of x_F for different intervals

of p_T^2, and also as functions of p_T^2 for different intervals of x_F. The asymmetries show a substantial dependence on x_F and some dependence on p_T^2. There is evidence for a correlation between x_F and p_T^2.

The asymmetry $A(x_F)$ integrated over p_T^2, and the asymmetry $A(p_T^2)$ integrated over x_F, are presented in Fig. 5. This figure shows asymmetries for all three types of hyperons. The results are also listed in Table 1 along with statistical and systematic errors.

We looked for systematic effects from the following sources:

- Event selection criteria;
- The minimum transverse energy in the calorimeters required in the event trigger;
- Uncertainties in calculating relative efficiencies for particle and antiparticle;
- Effect of the 2.5% K^- contamination in the beam.

The first two effects were found to be negligible. A significant error came from the spectrometer efficiencies, and these uncertainties are included as systematic errors in Table 1.

The effect of the K^- contamination in the beam was difficult to estimate as no data on hyperon asymmetries in K^- production in this x_F range existed. However, even for equal π^- and K^- production of Λ^0's (as opposed to $\overline{\Lambda}^0$'s) and 100% asymmetry for kaons (i.e., no $\overline{\Lambda}^0$ production), only a 1.5% change would occur in the final result. As for the π^- $(\bar{u}d)$ beam, no rise in the asymmetry in the positive x_F direction was expected since both $\Lambda^0(uds)$ and $\overline{\Lambda}^0(\bar{u}\bar{d}\bar{s})$ shared one valence quark with the $K^-(\bar{u}s)$ beam. Similarly, any rise in the $\Xi^-(dss) - \Xi^+(\bar{d}\bar{s}\bar{s})$ asymmetry should have been approximately the same as for a π^- beam since, in both cases, the Ξ^- hyperon shared one valence quark with the beam particle. Since the $\Omega^-(sss)$ was a leading particle for a K^- beam, in this case some asymmetry was expected in the forward x_F region. We noted the low K^- content of the beam and the low x_F of our data. In any event, no effect was evident. Thus we did not correct our measured values of asymmetry for possible effects of kaon contamination in the beam.

The asymmetry curves for Λ^0 and for Ξ^- cross over at $x_F \sim 0.02$. At larger positive x_F the Ξ^- asymmetry becomes considerably larger than that for Λ^0. The fact that both beam and target particles share one valence quark with the Ξ^- and none with the Ξ^+, would predict that the Ξ^- asymmetries rise with increasing $|x_F|$ in both positive and negative x_F regions, as observed in our data. In contrast, the Λ^0 shares two valence quarks with the target and only one with the beam particles, while the $\overline{\Lambda}^0$ only shares one with the beam. Consequently the $\Lambda^0 - \overline{\Lambda}^0$ asymmetry rises sharply for $x_F < 0$ and not for $x_F > 0$. The $\Omega^- - \Omega^+$ asymmetry appears to be constant. Notice that

neither the Ω^- nor the Ω^+ shares valence quarks with either the beam or target particles.

The observed positive asymmetry for Ω could arise, in part, from the associated production of kaons. This could also be the origin of the observed positive asymmetry near $x_F = 0.0$ for Ξ's and Λ's. Part of the associated production enhancement of baryons, as opposed to antibaryons, may come from the higher energy thresholds for the production of antibaryons. For production of hyperons, the conservation of strangeness requires only the associated production of one or more kaons. For production of an antihyperon, baryon number as well as strangeness must be conserved, requiring the associated production of at least two additional baryons, thus raising the energy thresholds and favoring particle over antiparticle production [6].

The behavior of the three asymmetries shown in Fig. 5 gives evidence for the leading particle effect. In the backward region ($x_F < 0$), a larger asymmetry is observed when there is a larger difference in the number of valence quarks in common with the target, for hyperon and antihyperon. Evidence for a similar effect in the production of $D^{\pm}$ mesons in the forward region ($x_F > 0$) was presented by the E791 collaboration [1] and others [13]. The E791 collaboration has also studied asymmetries in the production of $D_s^{\pm}$ [2] and $\Lambda_c^{\pm}$ [14]. However, leading particle effects for charmed hadrons typically occur at larger values of x_F than they do for strange hadrons.

The PYTHIA/JETSET [12] model describes only some features of our results, and those only qualitatively, as can be seen in Fig. 5. This model predicts small values of asymmetry for $x_F \sim 0$; this is in contrast with our results which range from 0.08 to 0.18 in this region. Our data show that, even in the central region, the asymmetries are not zero, and suggest that leading particle effects play an even larger role than expected as $|x_F|$ increases.

In summary we report the most precise, systematic study to date of the production asymmetry for Λ, Ξ, and Ω hyperons in a single experiment. The range of x_F covered, $-0.12 \leq x_F \leq 0.12$, allows the study of asymmetries in regions close to $x_F = 0$ for the first time in a fixed target experiment. Some evidence for possible correlations between x_F and p_T^2 is observed (see Figs. 3 and 4). Our results for particle-antiparticle asymmetries are consistent with the experimental results obtained by previous experiments [7,8] (see Table 2) but with smaller uncertainties. Our results can be described qualitatively in terms of the energy thresholds for the production of hyperons and antihyperons together with their associated particles and a model in which the recombination of valence and sea quarks in the beam and target particles contributes to the hyperon and antihyperon production in an asymmetrical manner [5].

We gratefully acknowledge the assistance of the staffs of Fermilab and of all

the participating institutions. This research was supported by the Brazilian Conselho Nacional de Desenvolvimento Científico e Tecnológico, CONACyT (Mexico), the U.S.-Israel Binational Science Foundation, the U.S. National Science Foundation and the U.S. Department of Energy. Fermilab is operated by the Universities Research Associates, Inc., under contract with the United States Department of Energy.

References

[1] E.M. Aitala et al. (E791 Collaboration), Phys. Lett. B 371 (1996) 157; G.A. Alves et al. (E769 Collaboration), Phys. Rev. Lett. 72 (1994) 812 and **72** (1994) 1946; M. Adamovich et al. (WA92 Collaboration), Nucl. Phys. B 495 (1997) 3.

[2] E.M. Aitala et al. (E791 Collaboration), Phys. Lett. B 411 (1997) 230.

[3] V.G. Kartvelishvili, A.K. Likhoded, and S.R. Slobospitskii, Sov. J. Nucl. Phys. **33** (1981) 434; R.C. Hwa, Phys. Rev. **D 51** (1995) 85; R. Vogt and S.J. Brodsky, Nucl. Phys. **B 478** (1996) 311; B.W. Harris, J. Smith, and R. Vogt, Nucl. Phys. **B 461** (1996) 181; G. Herrera and J. Magnin, Eur. Phys. J. **C 2** (1998) 477.

[4] L. G. Pondrom, Physics Reports, Vol. 122, Nos. 2 and 3 (1985) 57–172.

[5] J.C. Anjos, J. Magnin, F.R.A. Simão, and J. Solano, Proceedings of II Silafae, pg. 540, AIP Conf. Proc. No. 444 (1998), hep-ph/9806396; W.G.D. Dharmaratna and G.R. Goldstein, Phys. Rev. D 41 (1990) 1731.

[6] A. Capella, U. Sukhatme, C.I. Tan, and J. Tran Thanh Van, Phys. Rev. D 36 (1987) 109.

[7] S. Barlag et al. (ACCMOR Collaboration), Phys. Lett. B 325 (1994) 531.

[8] S. Barlag et al. (ACCMOR Collaboration), Phys. Lett. B 233 (1989) 522.

[9] S. Mikocki et al. (E580 Collaboration), Phys. Rev. D 34 (1986) 42; R.T. Edwards et al. (E415 Collaboration), Phys. Rev. D 18 (1978) 76; N.N. Biswas et al. (E002, E281, and E597 Collaborations), Nucl. Phys. B 167 (1980) 41; D. Bogert et al. (E234 Collaboration), Phys. Rev. D 16 (1977) 2098.

[10] J.A. Appel, Ann. Rev. Nucl. Part. Sci. **42** (1992) 367, and references therein; D.J. Summers et al. (E791 Collaboration), Proceedings of the $XXVII^{\rm th}$ *Rencontre de Moriond*, Electroweak Interactions and Unified Theories, Les Arcs, France (15-22 March, 1992) 417; E.M. Aitala, et al. (E791 Collaboration), EPJdirect **C 4** (1999) 1.

[11] S. Amato, *et al.*, Nucl. Instr. and Methods A 324 (1993) 535.

[12] Pythia 5.7 and Jetset 7.4. Physics Manual, CERN-TH-7112/93 (1993); H.U. Bengtsson and T. Sjöstrand, Computer Physics Commun **46** (1987) 43; T. Sjostrand, CERN-TH.7112/93 (1993).

[13] G.A. Alves et al. (E769 Collaboration), Phys. Rev. Lett. 77 (1996) 2388; G.A. Alves et al. (E769 Collaboration), Phys. Rev. Lett. 81 (1998) 1537; M. Adamovich et al. (WA82 Collaboration), Phys. Lett. B 305 (1993) 402.

[14] E.M. Aitala et al. (E791 Collaboration), submitted to Phys. Lett. B (2000), hep-ex/0008020.

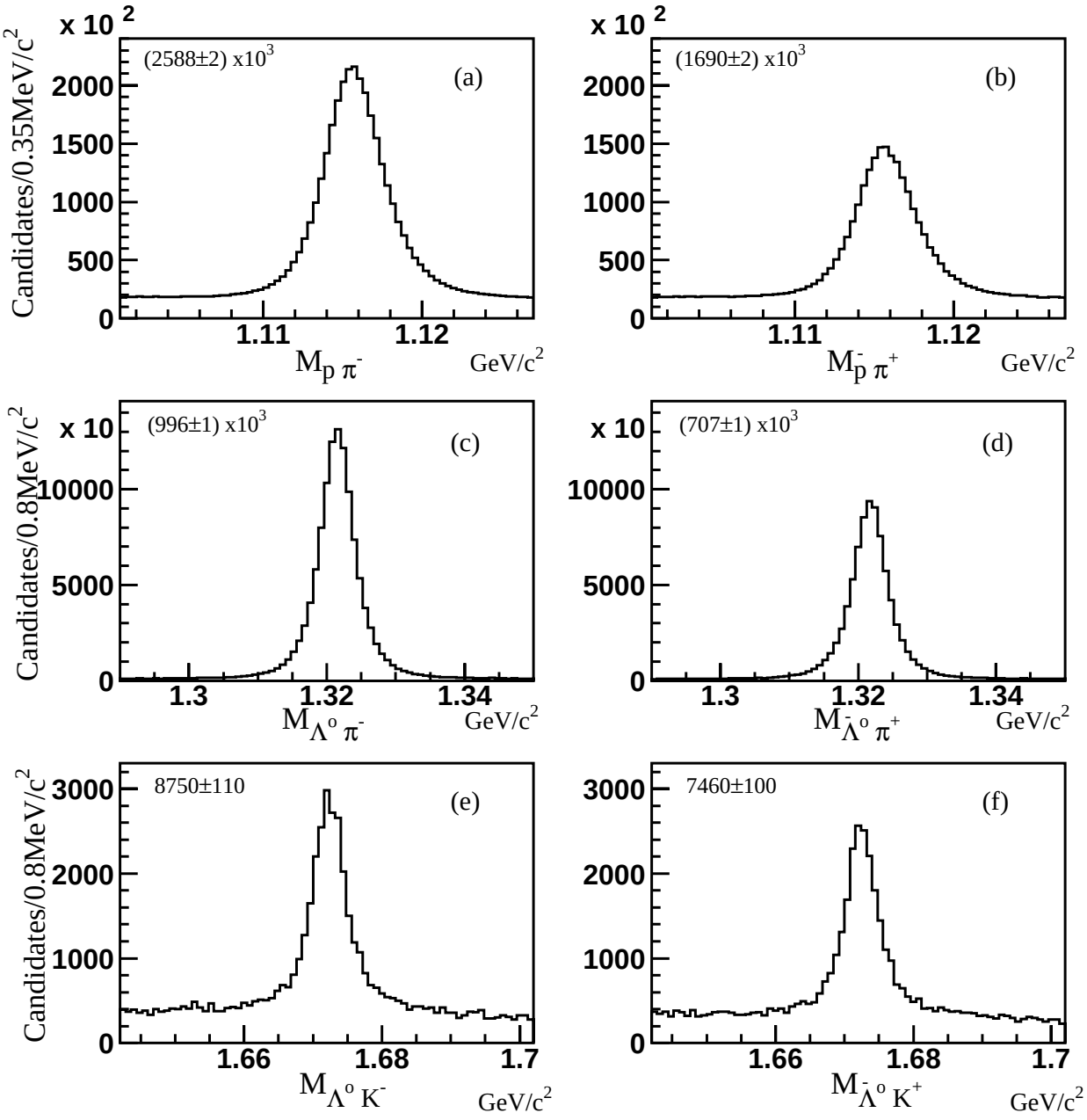

Fig. 1. Effective mass distributions for decay products of hyperons in events selected for this study and the corresponding signals with background subtracted. Plots correspond to (a) $\Lambda^0 \to p\pi^-$; (b) $\overline{\Lambda}^0 \to \overline{p}\pi^+$; (c) $\Xi^- \to \Lambda^0\pi^-$; (d) $\Xi^+ \to \overline{\Lambda}^0\pi^+$; (e) $\Omega^- \to \Lambda^0 K^-$ (f) $\Omega^+ \to \overline{\Lambda}^0 K^+$. The numbers and errors in the top corner of each plot come from the sum of the number of background subtracted events in the individual (x_F, p_T^2) bin fits.

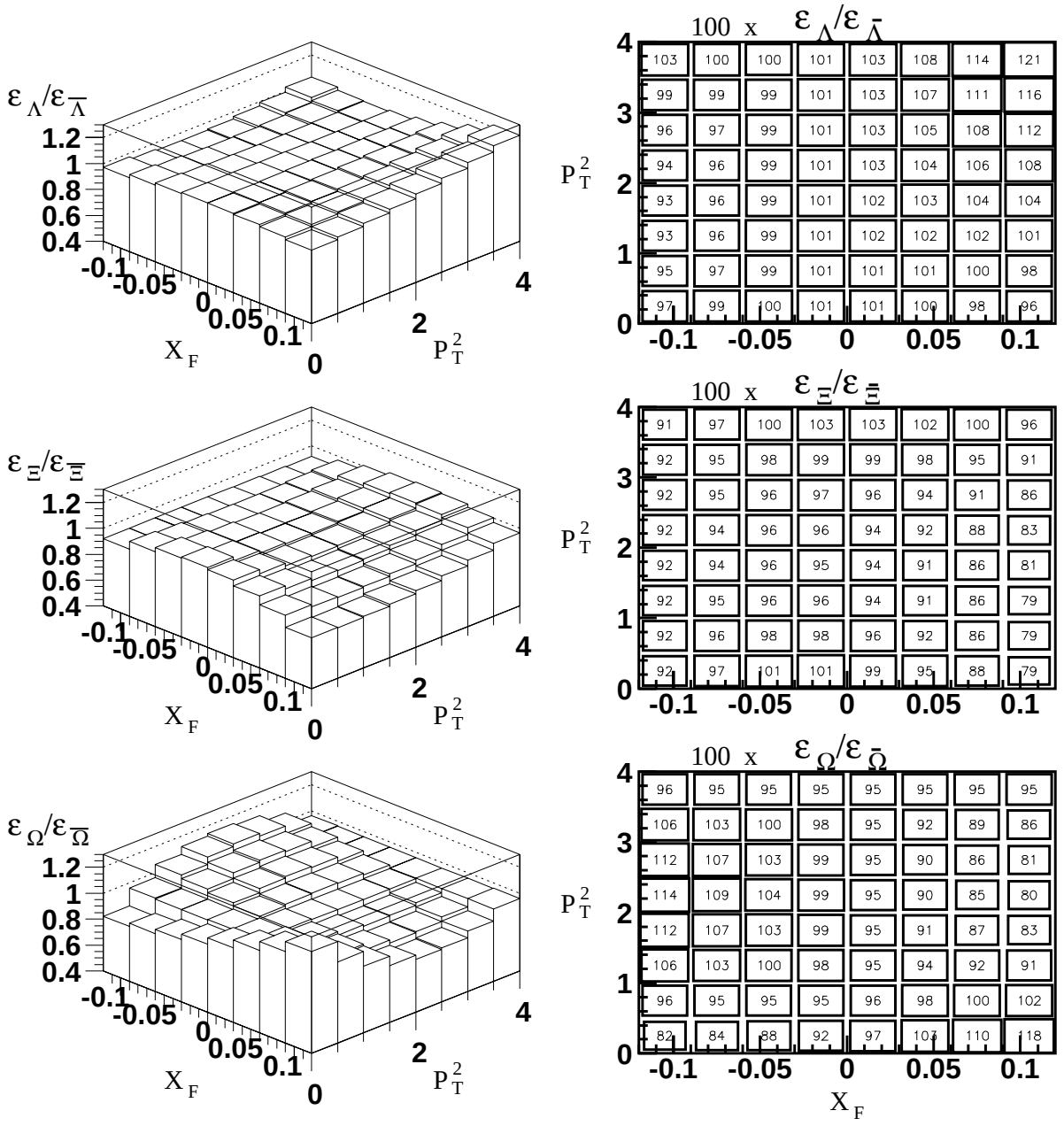

Fig. 2. Ratio of efficiencies as functions of x_F and p_T^2 for the three hyperons. The transverse momentum axes are in units of $(\mathrm{GeV}/c)^2$.

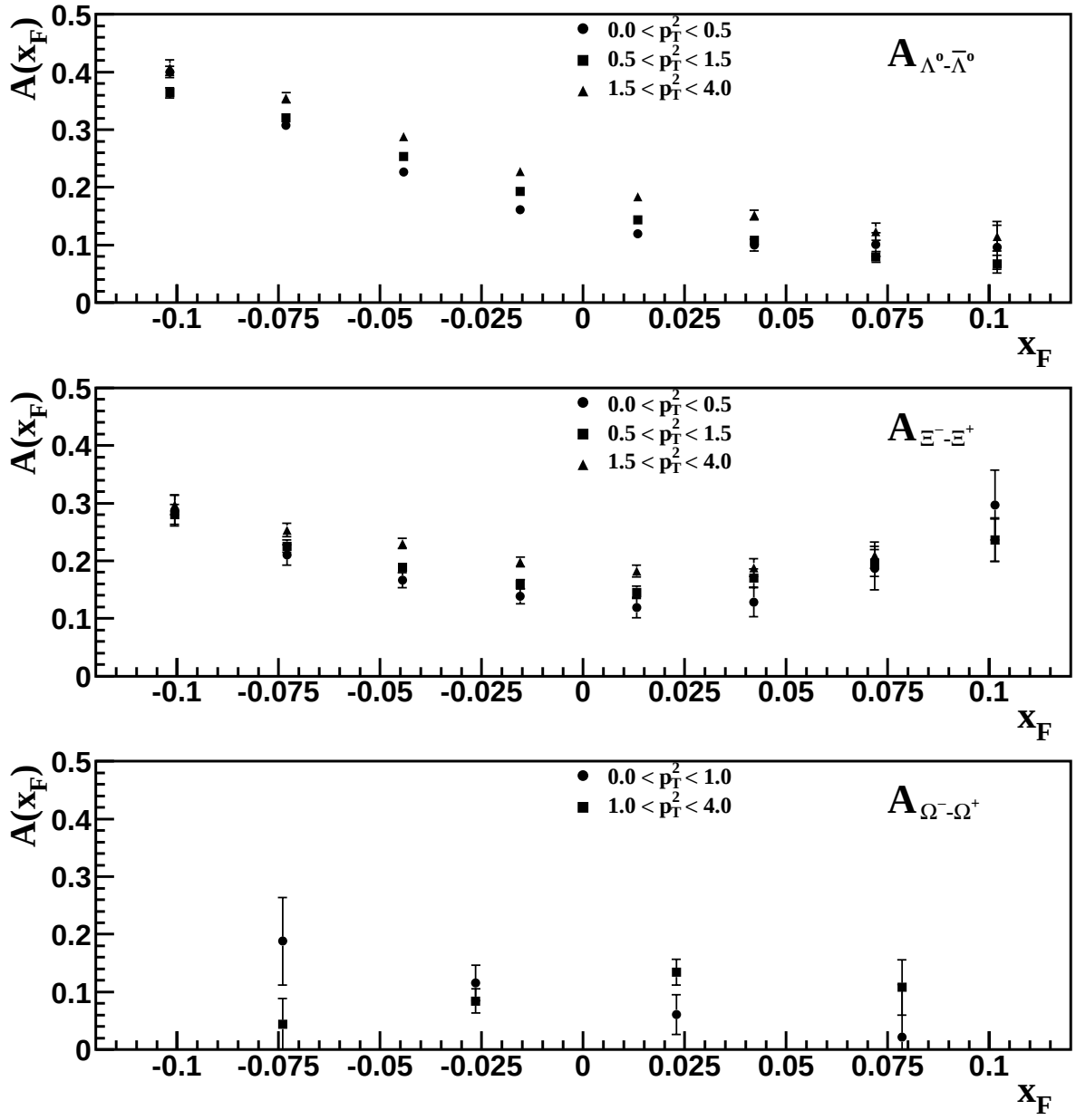

Fig. 3. $\Lambda^0 - \overline{\Lambda}^0$ (upper), $\Xi^- - \Xi^+$ (middle), and $\Omega^- - \Omega^+$ (lower) production asymmetries as a function of x_F in different p_T^2 regions.

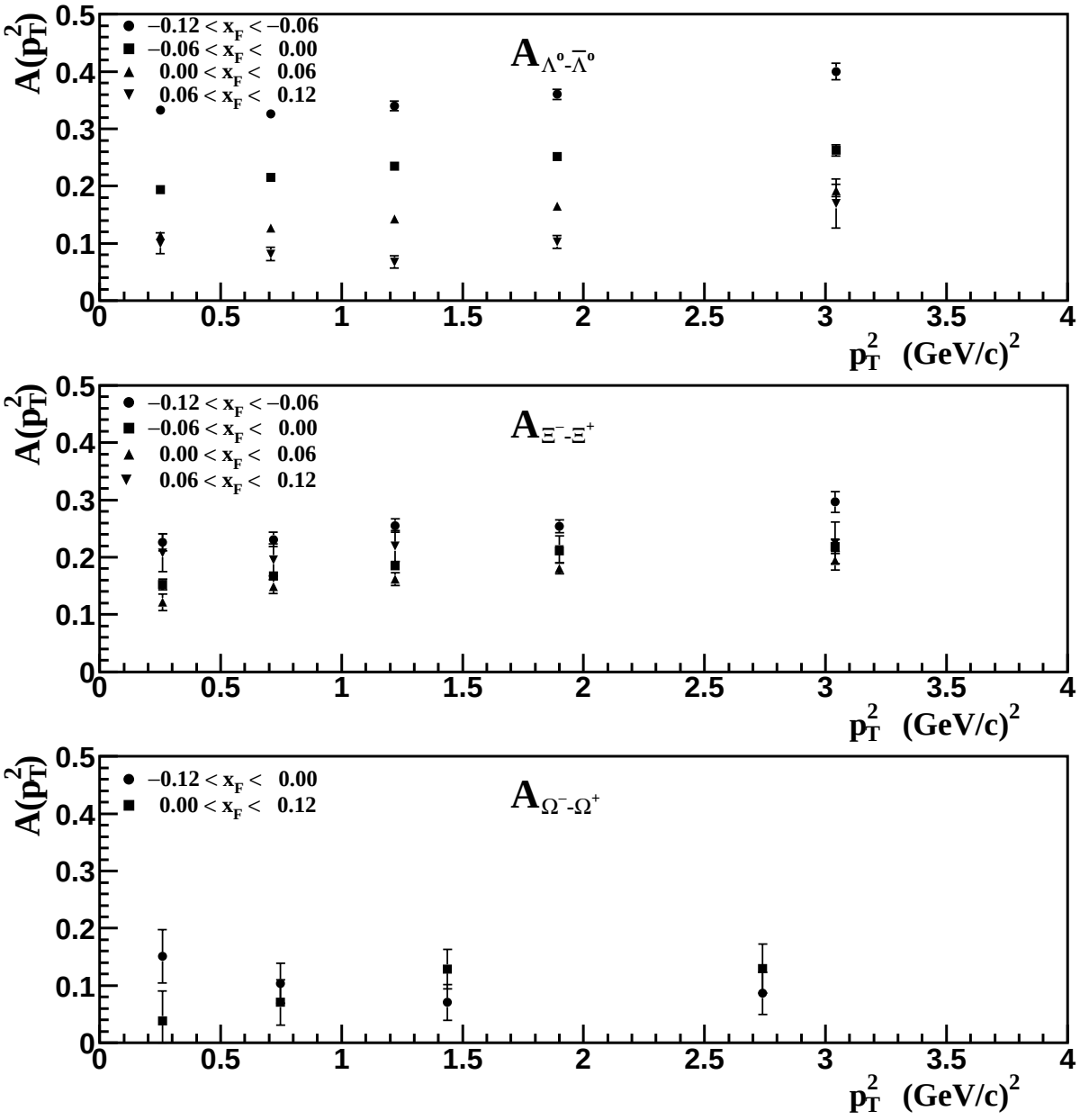

Fig. 4. $\Lambda^0 - \overline{\Lambda}^0$ (upper), $\Xi^- - \Xi^+$ (middle), and $\Omega^- - \Omega^+$ (lower) production asymmetries as a function of p_T^2 in different x_F regions.

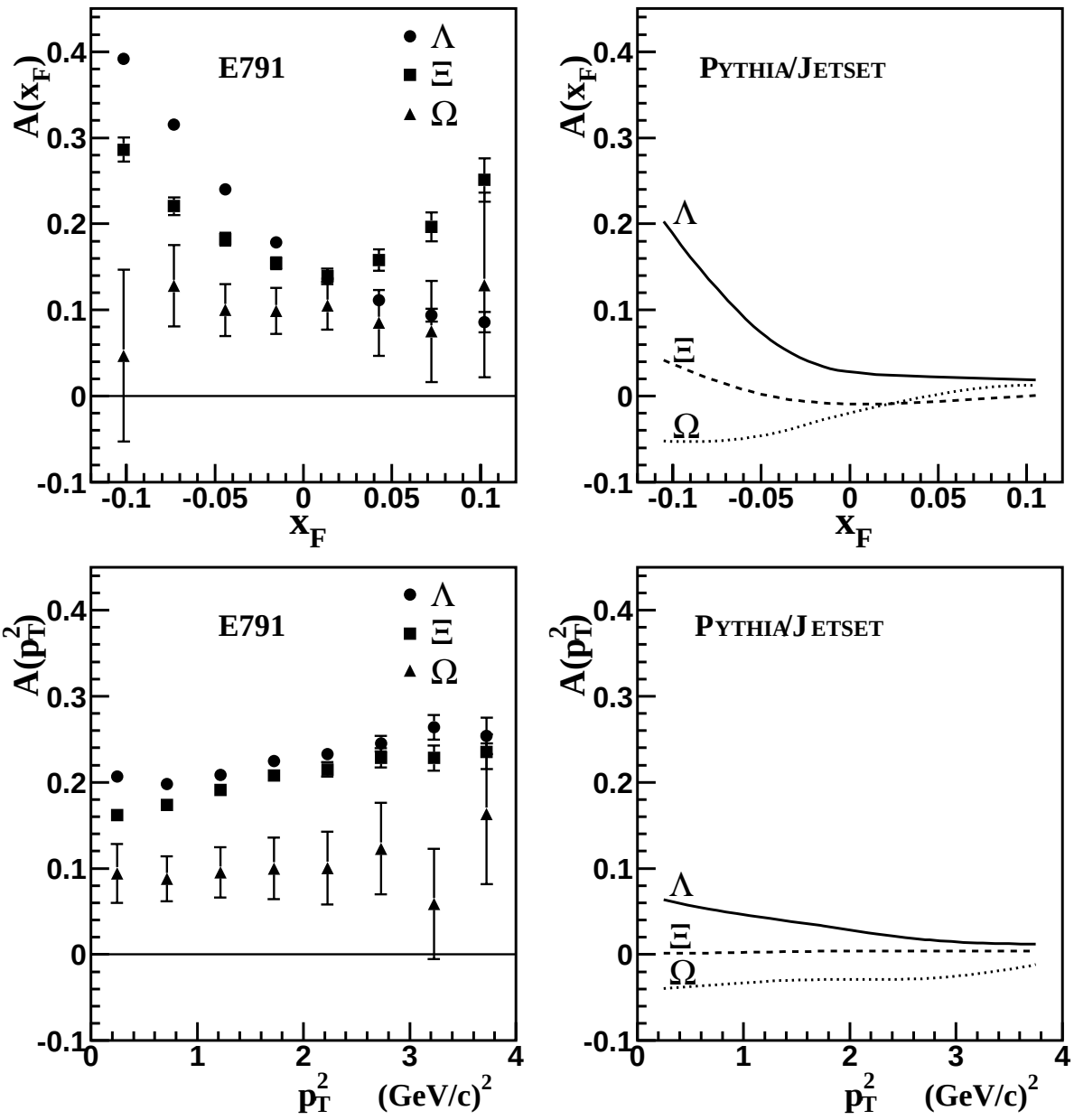

Fig. 5. Comparison among the asymmetries in the production of the three hyperons for the E791 data and PYTHIA/JETSET predictions. The error bars of the E791 data include the statistical and systematic uncertainties

Table 1
Final asymmetries of Λ, Ξ, and Ω showing the statistical plus systematical errors. The statistical errors given include those due to the number of observed events and the number of MC events. Typically, the error is dominated by the MC uncertainty.

x_F Region	$A_{\Lambda^0-\overline{\Lambda}^0} = \frac{\Lambda^0-\overline{\Lambda}^0}{\Lambda^0+\overline{\Lambda}^0}$	$A_{\Xi^- -\Xi^+} = \frac{\Xi^- -\Xi^+}{\Xi^- +\Xi^+}$	$A_{\Omega^- -\Omega^+} = \frac{\Omega^- -\Omega^+}{\Omega^- +\Omega^+}$
-0.12 – -0.09	$0.392 \pm 0.007 \pm 0.001$	$0.286 \pm 0.014 \pm 0.001$	$0.047 \pm 0.096 \pm 0.028$
-0.09 – -0.06	$0.315 \pm 0.005 \pm 0.001$	$0.220 \pm 0.010 \pm 0.001$	$0.128 \pm 0.046 \pm 0.005$
-0.06 – -0.03	$0.240 \pm 0.004 \pm 0.001$	$0.182 \pm 0.007 \pm 0.001$	$0.100 \pm 0.030 \pm 0.001$
-0.03 – 0.00	$0.179 \pm 0.002 \pm 0.001$	$0.154 \pm 0.007 \pm 0.001$	$0.099 \pm 0.027 \pm 0.002$
0.00 – 0.03	$0.136 \pm 0.002 \pm 0.001$	$0.139 \pm 0.009 \pm 0.001$	$0.106 \pm 0.028 \pm 0.001$
0.03 – 0.06	$0.111 \pm 0.005 \pm 0.001$	$0.158 \pm 0.012 \pm 0.001$	$0.085 \pm 0.038 \pm 0.005$
0.06 – 0.09	$0.094 \pm 0.008 \pm 0.001$	$0.196 \pm 0.017 \pm 0.001$	$0.075 \pm 0.058 \pm 0.011$
0.09 – 0.12	$0.086 \pm 0.012 \pm 0.003$	$0.250 \pm 0.025 \pm 0.001$	$0.129 \pm 0.106 \pm 0.018$
p_T^2 Region	$A_{\Lambda^0-\overline{\Lambda}^0} = \frac{\Lambda^0-\overline{\Lambda}^0}{\Lambda^0+\overline{\Lambda}^0}$	$A_{\Xi^- -\Xi^+} = \frac{\Xi^- -\Xi^+}{\Xi^- +\Xi^+}$	$A_{\Omega^- -\Omega^+} = \frac{\Omega^- -\Omega^+}{\Omega^- +\Omega^+}$
0.0 – 0.5	$0.206 \pm 0.002 \pm 0.001$	$0.162 \pm 0.007 \pm 0.001$	$0.094 \pm 0.034 \pm 0.001$
0.5 – 1.0	$0.198 \pm 0.002 \pm 0.001$	$0.173 \pm 0.006 \pm 0.001$	$0.088 \pm 0.026 \pm 0.001$
1.0 – 1.5	$0.209 \pm 0.003 \pm 0.001$	$0.191 \pm 0.005 \pm 0.001$	$0.095 \pm 0.029 \pm 0.001$
1.5 – 2.0	$0.224 \pm 0.003 \pm 0.001$	$0.207 \pm 0.006 \pm 0.001$	$0.099 \pm 0.036 \pm 0.001$
2.0 – 2.5	$0.233 \pm 0.006 \pm 0.002$	$0.215 \pm 0.008 \pm 0.001$	$0.100 \pm 0.042 \pm 0.003$
2.5 – 3.0	$0.245 \pm 0.008 \pm 0.005$	$0.229 \pm 0.011 \pm 0.001$	$0.123 \pm 0.052 \pm 0.011$
3.0 – 3.5	$0.264 \pm 0.011 \pm 0.009$	$0.228 \pm 0.015 \pm 0.001$	$0.080 \pm 0.062 \pm 0.017$
3.5 – 4.0	$0.254 \pm 0.015 \pm 0.015$	$0.235 \pm 0.020 \pm 0.001$	$0.163 \pm 0.080 \pm 0.019$

Table 2
Fully corrected production asymmetries of Λ, Ξ, and Ω integrated over three x_F regions. Errors are obtained by adding the statistical and systematic errors in quadrature. Results of ACCMOR [7,8] integrated over the range $0 \leq x_F \leq 0.35$ are shown for comparison.

	E791	E791	E791	ACCMOR
	$-0.12 \leq x_F \leq 0.12$	$-0.12 \leq x_F \leq 0$	$0 \leq x_F \leq 0.12$	$0 \leq x_F \leq 0.35$
$A_{\Lambda^0-\overline{\Lambda}^0}$	0.207 ± 0.001	0.242 ± 0.002	0.124 ± 0.002	0.119 ± 0.009 [7]
$A_{\Xi^- -\Xi^+}$	0.176 ± 0.004	0.186 ± 0.004	0.150 ± 0.007	0.130 ± 0.050 [8]
$A_{\Omega^- -\Omega^+}$	0.099 ± 0.013	0.098 ± 0.018	0.100 ± 0.021	0.107 ± 0.070 [8]